https://doi.org/10.31436/iiumej.v24i2.2803

3D COLLISION AVOIDANCE SYSTEM FOR UNMANNED AERIAL VEHICLE (UAV) WITH DECENTRALIZED APPROACH

MOHAMAD HANIFF HARUN[1,2,3]*, SHAHRUM SHAH ABDULLAH[1], MOHD SHAHRIEEL MOHD ARAS[3], MOHD BAZLI BAHAR[1,3] AND FARIZ ALI@IBRAHIM[3]

[1]Department of Electronic System Engineering,
Malaysia-Japan International Institute of Technology,
UTM KL Campus, Jalan Sultan Yahya Petra, 54100 Kuala Lumpur, Malaysia
[2]Faculty of Electric and Electronic Engineering Technology,
Universiti Teknikal Malaysia Melaka,
Hang Tuah Jaya, 76100 Durian Tunggal, Melaka, Malaysia
[3]Underwater Technology Research Group (UTeRG),
Center for Robotics and Industrial Automation (CERIA), Faculty of Electrical Engineering,
Universiti Teknikal Malaysia Melaka, 76100 Durian Tunggal, Melaka, Malaysia.

[*]Corresponding author: haniff@utem.edu.my

(Received: 23 March 2023; Accepted: 20 May 2023; Published on-line: 4 July 2023)

ABSTRACT: Unmanned aerial vehicles UAVs have been developed and refined for decades. Using an integrated software system, autonomous unmanned aerial vehicles (UAVs) perform missions automatically and return to a pre-programmed point. Malaysia has a lot of unoccupied airspace, yet autonomous UAV applications and research are still rare. In critical conditions, autonomous UAVs must deal with a variety of environmental and flight issues. This project involves a decentralized 3D collision avoidance system for an autonomous UAV. Ultrasonic, infrared, and laser rangefinders were chosen for the 3D collision avoidance system. The UAV's obstacle recognition and collision avoidance performance are also tested in four experiments. In various flight conditions, the 3D collision avoidance system can identify several material types and opacities by integrating selected rangefinders. Finally, the 3D collision avoidance system quickly reacts to obstacles in the X, Y, and Z axes.

ABSTRAK: Kenderaan udara tanpa pemandu (UAV) telah dibangunkan dan diperhalusi selama beberapa dekad. Menggunakan sistem perisian bersepadu, kenderaan udara tanpa pemandu (UAV) autonomi melaksanakan misi secara automatik dan kembali ke titik pra-diprogramkan. Malaysia mempunyai banyak ruang udara yang tidak berpenghuni, namun aplikasi dan penyelidikan UAV autonomi masih jarang berlaku. Dalam keadaan kritikal, UAV autonomi mesti menangani pelbagai isu alam sekitar dan penerbangan. Projek ini melibatkan sistem pengelakan perlanggaran 3D terpencar untuk UAV autonomi. Pencari jarak ultrasonik, inframerah dan laser telah dipilih untuk sistem pengelakan perlanggaran 3D. Prestasi pengecaman halangan dan pengelakan perlanggaran UAV juga diuji dalam empat eksperimen. Dalam pelbagai keadaan penerbangan, sistem pengelakan perlanggaran 3D boleh mengenal pasti beberapa jenis bahan dan kelegapan dengan menyepadukan pencari jarak terpilih. Akhir sekali, sistem pengelakan perlanggaran 3D bertindak balas dengan cepat terhadap halangan dalam paksi X, Y dan Z.

KEYWORDS: *decentralized 3D collision avoidance; unmanned aerial vehicle; rangefinder*

https://doi.org/10.31436/iiumej.v24i2.2803

1. INTRODUCTION

The IR 4.0 is increasing interest in autonomous UAVs. A UAV is an aerial vehicle that may be piloted from a distance [1]. UAVs are of use in military and civilian/commercial applications due to their wide range, inexpensive maintenance, quick deployment, mobility, and ability to hover [2]. The military uses UAVs for border security surveillance, reconnaissance, and target removal. Unmanned aerial vehicles are also used for search and rescue, parcel delivery, precision horticulture, and pharmaceutical transport. Multi-rotor drones, fixed-wing drones, single-rotor helicopters, and fixed-wing Vertical Take-Off and Landing (VTOLs) are the four main drone types, as shown in Fig. 1.

The fact remains that each key drone type has its own benefits and drawbacks. For example, multi-rotor drones may hover due to their vertical direction drive framework, while single-rotor helicopters can hover and rotate due to their vertical direction drive framework. To put it another way, this type of aerial vehicle has slow movement speeds and requires extra energy to fulfil tasks [3]. However, fixed-wing drones and fixed-wing hybrid VTOLs can travel long distances due to their propulsion system and aerodynamic surfaces. Fixed-wing VTOLs (vertical takeoff and landing) can launch and land vertically without a runway [3]. However, fixed-wing drones have many drawbacks. Fixed-wing aircraft require a lot of airspace to maneuver and direct themselves. Other than that, the aerodynamic wing surfaces produce lifting power through air impacts.

UAVs have both military and commercial uses. They must be built to work in difficult settings, such as huge open spaces, dense tree clusters, or rocky mountain slopes [4]. As a result, UAVs will struggle to achieve their missions in these hostile environments. Outdoor operation of UAVs is even more problematic due to GPS errors, poor communication, and bad weather [5]. Sensors enable UAVs to scan their surroundings and avoid collisions. Collecting accurate environmental data is important to avoiding crashes and completing the mission. Due to the increasing utilization of multi-UAV cooperative operations, 3D collision avoidance is crucial. When functioning centrally, an unmanned aerial vehicle assesses all colleagues' inputs and outputs to avoid collisions. While a central communication hub is beneficial, it is difficult to expand [6-8]. Decentralized systems can also handle more UAV teams in congested situations. These are more stable and robust.

Malaysia is believed to be falling behind in aerial vehicle research and development compared to countries like the US, China, and Iran. Limitations include lack of aeronautical knowledge, high sensor and communication system costs, and limited airspace. To boost Malaysia's aeronautics industry, aerial vehicle research and development must continue. Currently, only a few Malaysian aerospace companies are researching and developing autonomous UAVs to solve industrial and military concerns.

In many situations, rapid deployment of aerial vehicles can change a crisis situation into a non-critical situation since they can gather information faster than humans. Wildfires, medication delivery, crime fighting, and search and rescue are examples [9]. Wildfires, like the 2019 Amazon rainforest fires, can erupt at any time throughout the dry season [10]. Also, the Amazon rainforest covers 5.5 million km^2, making human patrolling and scouting impractical. Using flying vehicles to monitor the Amazon rainforest could help limit the damage and mortality caused by wildfires.

https://doi.org/10.31436/iiumej.v24i2.2803

Fig. 1: Types of drones.

2. THEORETICAL BACKGROUND

Numerous theories and principles must be explored and incorporated into the design and development of the unmanned aerial vehicle with decentralized 3D collision avoidance system. Aerodynamic forces, center of gravity (CG), and time of flight (ToF) are all significant theories and principles of flight.

2.1 Aerodynamic Force

All aircraft in flight are subjected to the forces of thrust, drag, lift, and weight. Understanding how these forces interact and utilizing power and flight controls to manage them is critical for flight. Thrust, drag, lift, and weight are the four forces that act on an airplane in level, unaccelerated flight [11]. These are the terms that are used to describe them:

a) Thrust—the force applied forward by the engine/propeller or rotor. It opposes or overcomes drag. By and large, it acts perpendicular to the longitudinal axis.

b) Drag—a rearward, retarding force created by the wing, rotor, fuselage, and other projecting items disrupting airflow. Drag, on the other hand, opposes thrust and acts in the opposite direction of the relative wind.

c) Lift—is a force generated by the dynamic action of the air on the airfoil that acts perpendicular to the flight path through the center of lift (CL) and perpendicular to the lateral axis. Lift opposes the downward force of weight in level flight.

d) Weight—the total weight of the aircraft, crew, fuel, and cargo or baggage. Weight is a force that acts as a drag on the aircraft due to the force of gravity. It acts vertically downward through the aircraft's center of gravity (CG) and opposes lift.

The sum of these opposing pressures is always zero in steady flight. According to Newton's Third Law, there can be no unbalanced forces in steady, straight flight, because every action or force has an equal but opposing response or force. This is true regardless of whether you are flying level or ascending or descending.

This is not to say that the four forces are equal. This signifies that the opposing forces are equivalent to one another and hence cancel out their effects. In Fig. 2(a), the thrust, drag, lift, and weight force vectors appear to be identical in magnitude. The conventional explanation claims (without specifying) that thrust equals drag and weight equals lift. While this statement is true, it might be misleading. It should be known that the opposing

https://doi.org/10.31436/iiumej.v24i2.2803

lift/weight forces are equal in straight, level, unaccelerated flight. Additionally, they are greater than the opposing thrust/drag forces, which are equal only to one another.

This revision of the conventional "thrust equals drag; lift equals weight" formula explains that during climbs and slow flight, a component of force is directed upward and functions as lift, while a piece of weight is directed backward in the opposite direction of flight and acts as drag. In sluggish flight, thrust is directed upward. However, because the aircraft is in level flight, weight has no effect on drag, as illustrated in Fig. 2(b).

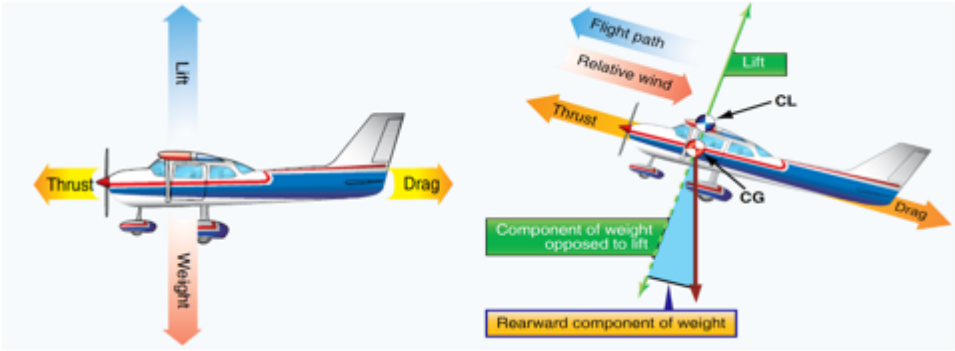

(a) (b)

Fig. 2: (a) Relationship of forces acting on an aircraft (b) Force vectors during a stabilized climb.

2.2 Centre of Gravity (CG)

A body in a gravitational field has an unlimited number of particles of varying sizes, each with its own weight. The total weight of the body is the resultant parallel force system created by those weights [12]. Moreover, when the gravitational field is uniform over a body, the center of gravity is also the center of mass. The UAV's center of gravity influences the UAV's balance while in flight. To improve overall flying performance and minimize any instability issues, the UAV's center of gravity must be on the same horizontal plane as the propellers.

2.3 Vibration

Vibration is the oscillating motion of a system or body of attached bodies [13]. Free vibration and forced vibration are the two main types of vibration. Forced vibration is created by an external periodic or intermittent force, whereas free vibration is caused by gravitational or elastic restoring forces. A UAV's vibrations come from its aerodynamic, mechanical, and flying motions. Due to electronic components like flight controllers, inertial measurement units (IMUs), and sensors are susceptible to vibrations, multirotor UAVs have motor-propeller produced vibrations. It is also vital to consider vibrations because a built UAV vibrating at its normal frequency would be disastrous. So, it is critical to isolate electrical components from vibrations and limit UAV vibrations as much as feasible.

2.4 Time of Flight (ToF)

The Time-of-Flight concept measures the distance between a sensor and an item by the time it takes for a signal to travel from the sensor to the object and back. The Time-of-Flight principle works with several signals (carriers), the most prevalent being sound and light [14]. Light is the carrier for TeraRanger sensors because it combines speed, range, weight,

and eye-safety. As a result, infrared sensors perform better than other distance sensors of similar size and weight.

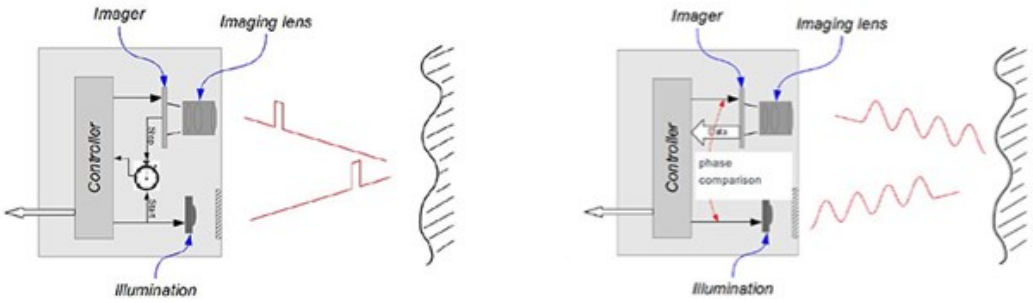

(a) (b)

Fig. 3: (a) Direct ToF (b) Indirect ToF.

Time-of-Flight (ToF) sensors detect distances by measuring the time it takes photons to travel from the sensor's emitter to a target and back. As illustrated in Fig. 3, both indirect and direct ToF have particular advantages. Both can measure a pixel's intensity and distance. Direct ToF sensors give out nanosecond-long light pulses and time how long it takes for some of the light to return. Indirect ToF sensors use continuous modulated light to calculate the distance to objects. The object distance from the sensor can be calculated using Eq. 1, where d is the object distance and c is the sound or light speed.

$$d = \frac{c \times ToF}{2} \tag{1}$$

3. METHODOLOGY

This section contains a mechanical description and the concerns related to the design of the fuselage, landing gear, and propulsion system are described in detail. The electrical and electronic description includes in-depth discussions of the thought processes behind and justifications for the choice of components including the power supply, ESC, flight controller, RC transmission, and range finder. Finally, the experimental procedures are presented, including the setup of all four experiments.

3.1 Mechanical Part - Fuselage

SolidWorks is used to design the multirotor fuselage. The fuselage design defines the type of multirotor aircraft, such as the hexa-copter depicted in Fig. 4(a). Thus, multirotor aircraft have 6 motors and 6 propellers for propulsion. The extra two motors in the Hexa X rotor arrangement provide more lift force. A hexa-copter has higher stability and can continue to fly even if one of its motors fails. Also, the bare fuselage design is more convenient and versatile for research and development. These motor mounts are colored differently from the other motor mounts to show the multirotor aircraft's heading. The fuselage is also constructed such that the motor arms may be stored and transported easily. The multirotor aircraft also features a cargo mechanism at the bottom for extra electronics or sensors.

To build the multirotor aircraft, the SolidWorks file of the bottom plate is exported as a drawing exchange format (DXF) file. This ensures the bottom plate is accurate and closely

matches the drawing. The carbon fiber tube is cut to the desired length using a grinder, where the intended motor-to-motor length is 685 mm.

3.2 Mechanical Part - Landing Gear

Similarly, SolidWorks is used to design the multirotor aircraft landing gear, which is shown in Fig. 4(b). This style of landing gear also allows for extra cargo area. The landing gear must be designed to support the overall weight of the multirotor aircraft plus any additional payloads. The landing gear can also be retracted horizontally for storage and transit.

Similar to the fuselage, the landing gear is made from carbon fiber plates and tubes, as seen in Fig. 4(b). The desired payload height clearance from the ground is 180 mm.

(a) (b)

Fig. 4: (a) Fuselage design (b) Landing gear.

3.3 Mechanical Part - Propulsion System

The mechanical components of a multirotor aircraft propulsion system include BLDC motors and propellers. BLDC motors and propellers for multirotor aircraft must be chosen based on the above requirements and the aircraft's overall takeoff weight. The weight of the multirotor aircraft is the key element impacting the BLDC motor choices. To reach the 2:1 thrust to weight ratio, the motors' total thrust must be at least twice the aircraft's entire takeoff weight [15]. The required motor thrust can also be determined using Eq. 2 from [16].

$$Thrust = \frac{(Total\ takeoff\ weight\ of\ aircraft) \times 2}{Number\ of\ motors} \tag{2}$$

The datasheet for a BLDC motor frequently includes the motor's thrust. Important information such as Kv ratings (RPM per supplied volt) and current ratings (maximum current drawable safely) are also included in the datasheet [17]. Additionally, to maximize motor efficiency, most BLDC motors recommend a propeller size and design. The multirotor aircraft constructed for this project is expected to weigh 3 kg in total. Tarot 4108 Brushless DC was finally selected. Six lithium-ion batteries (25.2 V), a 380 Kv motor with 1 kg of torque, and 1355 carbon fiber propellers were also selected. The UAV is 13 inches in diameter and has a 5.5-degree pitch. Therefore, the multirotor should include axial propulsion, puller configuration, and two-blade propellers for better performance.

https://doi.org/10.31436/iiumej.v24i2.2803

3.4 Electrical and Electronic Part – Power Supply

A multirotor aircraft's power supply is chosen to meet the propulsion system's voltage and current needs before being stepped down to meet the electronics components' voltage and current requirements. After settling on the motors and propellers, the series and parallel configuration of battery cells can be estimated. This is because one 18650 Li-ion cell delivers 4.2 V when completely charged and may safely draw up to 20 A (depending on the model). For example, to provide 24 V for the motors, at least 6 cells must be connected in series. Batteries are rated in mAh and C, where mAh is the maximum power stored and C is the rate of discharge relative to maximum capacity. According to Eqs. 3 and 4 from [18], a 2000 mAh Li-ion cell at 10 C may discharge at 20 A for 6 minutes.

$$I = Q \times C \tag{3}$$

$$Discharge\ time\ (minutes) = \frac{I}{C} \times 60 \tag{4}$$

Hence, the multirotor aircraft power supply will be LG HG2 3000 mAh 20 C 18650 Li-ion batteries (6S4P) as shown in Fig. 5(a) with a total capacity of 12000 mAh and a maximum voltage of 25.2 V. With this Li-ion battery combination, the motors can run for 12 minutes at maximum discharge current of 20 A. Because the motor can only draw 12.4 A at full throttle, the multirotor aircraft can only fly for 20 minutes. Nickel strips are used to spot weld the Li-ion cells into 6S4P arrangement.

3.5 Electrical and Electronic Part – Electronic Speed Control (ESC)

The ESC controls the motor speed of the multirotor aircraft, affecting the thrust force generated. The key problem in selecting an ESC is that it can handle the voltage and current draw from the power supply to the BLDC motors at full throttle. As indicated in Fig. 5(b), the multirotor aircraft ESC chosen is the HobbyWing XRotor-40A. A safety factor larger than 2 means the ESC's continuous current rating is substantially higher than the motors' maximum current demand.

3.6 Electrical and Electronic Part – Flight Controller

The flight controller of a multirotor aircraft receives input signals and converts them to output signals for the motors. So, one way to find a good flight controller is to look at its specs. The Pixhawk 2/Cube flight controller was chosen for the multirotor aircraft since it is open source and popular among UAV developers. The Cube also has a double redundant microprocessor, triple redundant IMU, and can accommodate up to three GPS modules. The Cube's (I/O) ports are also attached to a carrier board that can integrate with the Intel® Edison single board computer. It also includes 14 PWM pins, 8 of which have a failsafe and manual override.

Thus, redundant components in The Cube ensure that the flight controller does not fail. The carrier board also allows for easy attachment of sensors and other electronic components to the flight controller. Because Pixhawk 2 is an OSH, the dimensions and CAD model of the flying controller depicted in Fig. 5(c) are simply obtained. So, the flight controller may be exactly positioned in the multirotor center to ensure accurate IMU and accelerometer data.

3.7 Electrical and Electronic Part – DC Transmission

The multirotor aircraft uses RC transmission to receive radio signals from the transmitter. The transmission range and frequency are important factors to consider when

choosing an RC transmission system. The TTSRC X9 Remote Control 2.4 G 9CH Transmitter with Receiver X9D is chosen for manual mode since it has a transmission range up to 1 km and runs at 2.4 GHz. In autonomous mode, the 3DR 100 mW Radio Telemetry is chosen due to its 1.5 km transmission range and 915 MHz transmission frequency, as seen in Fig. 5(d) and 5(e). Moreover, both transmitting frequencies are legal.

Fig. 5: (a) Li-ion battery (b) ESC XRotor-40A (c) Pixhawk 2 CAD model (d) TTSRC X9 (e) 3DR radio telemetry

3.8 Electrical and Electronic Part – Rangefinder

The primary purpose of rangefinders is to determine the distance between an object and the rangefinder, but they are also utilized in this project to identify obstacles and avoid collisions. Table 1 compares several types of rangefinders.

Table 1: Comparison between rangefinders

Parameters	Ultrasonic Sensor	Infrared sensor	LiDAR sensor
Manufacturer	WAVGAT	SHARP	Benewake
Model	GY-US42V2	GP2Y0A710K0F	TFMini
Medium	Ultrasound	Infrared	Laser
Communication interface	Serial UART	Analog	Serial UART
Distance measuring range	20 cm ~ 720 cm	100 cm ~ 550 cm	30 cm ~ 1200 cm

To construct the decentralized 3D collision avoidance system, all of the rangefinders listed in Table 1 will be employed for sensor fusion, allowing the advantages of each rangefinder to outweigh the shortcomings of the others. Additionally, several simulations

and experiments will be undertaken to determine each rangefinder's performance in a variety of different environments.

3.9 Electrical and Electronic Circuit Diagram

Figure 6(a) illustrates the relationships between electrical components that are necessary for the building of the multirotor aircraft circuit diagram depicted in Fig. 6(b). The circuit schematic is created using Fritzing software to aid in the rapid and exact production of the electrical and electronic system.

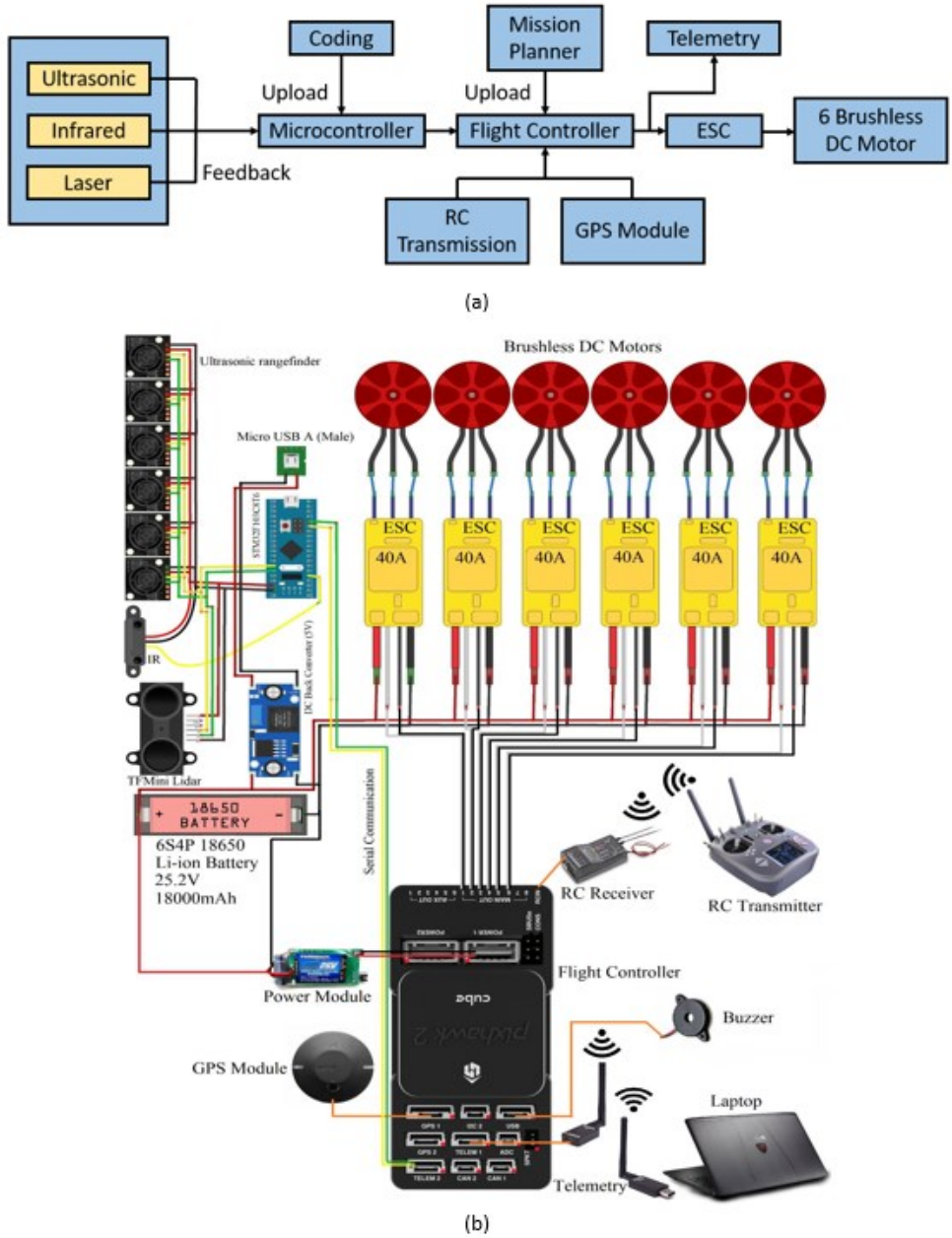

Fig. 6: (a) Electronic components relations, (b) Multirotor aircraft circuit diagram.

Multiple GPIO pins are available on microcontrollers and single-board computers to read analogue and digital inputs from sensors and to output analogue and digital voltage signals. This is to respond to the mobile robot's continually changing electrical requirements. The

microcontroller is used to read data from ultrasonic sensors that generate and receive digital signals. Additionally, through Universal Asynchronous Receiver and Transmitter (UART) connectivity, the single-board computer receives GPS coordinates from the GPS Module. Additionally, single-board computers are utilized to get photographs of railway track defects and video recordings of the railway track from cameras using serial connection protocol. C++ and Python will be used to program the microcontroller and single-board computer, respectively.

3.10 Experimental Procedures

Various experiments are conducted to obtain the required results to achieve the project's objectives. The results are based on the specific performance index to determine the success of the research. One of them is the percentage rate of obstacle detection based on the sensor fusion algorithm. This parameter is essential to show how quickly the system detects obstacles and the percentage of successful detection. The other parameter is the reaction time for the system to perform collision avoidance when an obstacle is detected. The reaction time is vital to ensure the system's robustness in all situations. Four experiments will be conducted to evaluate all the performance parameters for the system.

A. Experiment 1: Obstacle Detection on Multiple Type and Opacity of Material Test

Objective : To measure and determine the capabilities for obstacle detection on multiple type of material based on LiDAR, Sonar, and IR sensors

Parameters : Manipulated Variable: Type of rangefinder and material

Responding Variable: Detection of obstacle

Apparatus : White polystyrene, cotton hoodie, clear plastic, translucent plastic, wooden plank, black box and rangefinders

Procedure :

1. Ultrasonic, laser, and infrared rangefinders are positioned at a fixed distance from the wooden plank.
2. The microcontroller controlling the rangefinders is programmed to obtain the distance between the rangefinders and obstacle.
3. The distance obtained is recorded and compared with the fixed distance set between the rangefinders and obstacle.
4. Step 1 to 3 is repeated by changing the type of material to wooden plank, cotton hoodie, clear plastic, translucent plastic, white polystyrene and black box.
5. The results obtained are tabulated in table form.

B. Experiment 2: Obstacle Detection Range in Different Environments Test

Objective : To verify and evaluate the obstacle detection range for each type of rangefinder in various environments.

Parameters : Manipulated Variable: Flight environment.

Responding Variable: Obstacle detection range of rangefinder

Apparatus : Wooden plank, rangefinders, and multirotor aircraft

Procedure :
1. Ultrasonic, infrared, and laser rangefinders are mounted at the same position on the multirotor aircraft.
2. Multirotor aircraft is set up in a sunny environment.
3. The wooden plank is positioned at a fixed distance of 10m from the multirotor aircraft.
4. The distance between the wooden plank and multirotor aircraft is decreased to 9 m, 8 m, 7 m, 6 m, 5 m, 4 m, 3 m, 2 m, and 1 m.
5. The readings of the rangefinders are recorded.
6. Step 2 to 6 is repeated by setting up the multirotor aircraft in a cloudy environment and a night environment.
7. The results obtained are tabulated in table form.

C. Experiment 3: Collision Avoidance Reaction Time Test

Objective : To measure and study the reaction time of the multirotor aircraft on collision avoidance.

Parameters : Manipulated Variable: Velocity of incoming multirotor aircraft

Responding Variable: Reaction time of multirotor aircraft

Apparatus : Rangefinders, radio controller, telemetry, laptop, and multirotor aircraft

Procedure :
1. Multirotor aircraft with rangefinders mounted at forward facing position is set up at an empty and open field.
2. Mission Planner is launched on laptop and the flight path of the multirotor aircraft is planned.
3. The flight controller is configured to record the velocity of multirotor aircraft, rangefinder readings, and throttle level of each BLDC motor.
4. The multirotor aircraft took off manually in position hold mode using a radio controller and was controlled to move at a direction parallel to the surface obstacle at a speed of 2 m/s.
5. The data logged in graph form is tabulated in table form.
6. Step 4 to 6 is repeated by changing the speed of the multirotor aircraft to 4 m/s and 6 m/s.

D. Experiment 4: 3D Collision Avoidance Test

Objective : To evaluate and demonstrate the capability of the multirotor aircraft on 3D collision avoidance.

Parameters : Manipulated Variable: Position of obstacles.

Responding Variable: Collision avoidance of multirotor aircraft

Apparatus : Wooden plank, rangefinders, telemetry, laptop, and multirotor aircraft

Procedure :

1. Multirotor aircraft with mounted rangefinders is set up at an empty and open field.
2. Mission Planner is launched on laptop and the flight path of the multirotor aircraft is planned.
3. The multirotor aircraft took off in autonomous mode and executed the flight path planned.
4. Wooden plank is introduced along X-axis, Y-axis and Z-axis of the multirotor aircraft.
5. The reaction of the multirotor aircraft is observed and recorded.
6. The observations obtained are tabulated in table form.

4. RESULTS AND DISCUSSIONS

Results are based on the design of the multirotor aircraft and the 4 real experiments are conducted using the proposed multirotor aircrafts throughout this research.

4.1 Design of Multirotor Aircraft

As seen in Fig. 7(a) and 7(b), the built multirotor aircraft includes the following characteristics: Hexa X, typical fixed skid landing gear, two blade propellers, puller arrangement, and axial propulsion. Due to the cylindrical form of the motor arm, motor mount, and landing gear, clamping is needed to secure them in place; drilling a hole through the carbon fiber tube will reduce its strength. Silicon rubber dampers are installed on the carbon fiber tube that will come into touch with the ground to absorb impact forces on the landing gear system. The 6S4P 18650 Li-ion battery pack is arranged in Fig. 7(c), and it is designed to be sealed using a non-conductive waterproof sealing tape.

These dimensions are critical because they reflect the multirotor aircraft's virtual cylinder dimension for 3D collision avoidance. Thus, the width of the multirotor aircraft with propellers and the height of the multirotor aircraft with battery pack are utilized to establish the proportions of the virtual cylinder for 3D collision avoidance. As a result, the virtual cylinder has a diameter of 1014.7 mm and a height of 300.36 mm as shown in Table 2, which is used to construct a 3D collision avoidance system.

4.2 Obstacle Detection on Multiple Types and Opacity of Material Test

The performance of the collision avoidance system for multirotor aircraft is directly affected by the performance of the several rangefinder types on identifying multiple types

and opacity of material. This experiment will also assess each rangefinder's ability to detect obstacles. Table 2 lists the findings.

As shown in Table 3, ultrasonic sensors can successfully detect all materials used. Also, both laser and infrared rangefinders can detect all materials except transparent materials like clear plastic where incorrect readings occur. Contrary to expectations, ultrasonic sensors were able to detect soft materials like cotton hoodies with ease. However, humans typically wear cotton-based clothes, thus it is critical that the rangefinder utilized can detect it.

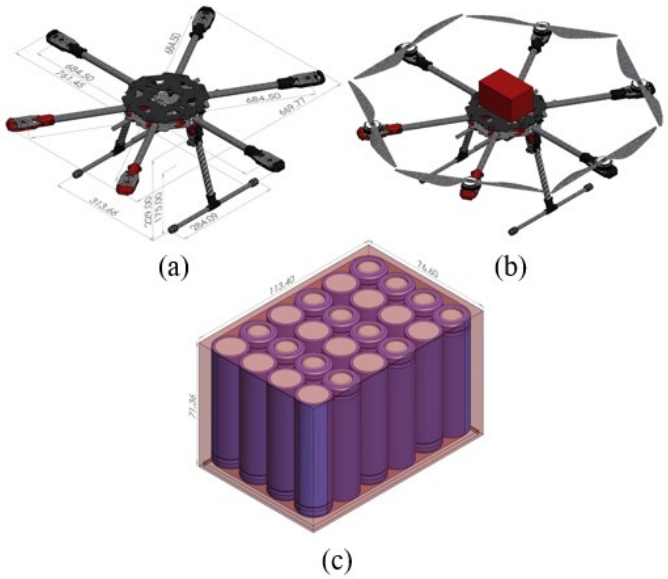

Fig. 7: (a) Multirotor aircraft frame design, (b) Modelling of multirotor aircraft design, (c) Modelling of 18650 Li-ion battery pack.

Table 2: Dimension of multirotor aircraft

Dimension	Length (mm)
Motor to motor length	684.50
Breadth (Without propellers)	669.77
Width (Without propellers)	761.45
Height (Without battery pack)	229.00
Breadth (With propellers)	922.99
Width (With propellers)	1014.70
Height (With battery pack)	300.36

Because laser and infrared rangefinders use light to measure distance between objects and the rangefinder, they have trouble identifying transparent materials. Light does not reflect from clear plastic since it is transparent and has low reflectivity. However, when using translucent materials such as translucent plastic, both the laser and infrared rangefinder may detect it due to the material's reflection.

Thus, the advantages of the ultrasonic rangefinder over laser and infrared rangefinder can be exploited to overcome the disadvantages. However, ultrasonic rangefinders have drawbacks including loud readings and limited obstacle detection range that can be overcome by laser and infrared rangefinders.

https://doi.org/10.31436/iiumej.v24i2.2803

Table 3: Obstacle Detection on Multiple Type and Opacity of Material Test

Type of Material	Material Used	Type of Rangefinder (RF)					
		Ultrasonic RF		Infrared RF		Laser RF	
		Detection	Observation	Detection	Observation	Detection	Observation
Hard	Wooden plank	√	Good	√	Good	√	Good
Soft	Cotton hoodie	√	Good	√	Good	√	Good
Transparent	Clear plastic	√	Good	X	Bad	X	Bad
Translucent	Translucent plastic	√	Good	√	Good	√	Good
Bright	White polystyrene	√	Good	√	Good	√	Good
Dark	Black box	√	Good	√	Good	√	Good

Table 4: Obstacle Detection Range in different Flight Environments Test Using Ultrasonic, Infrared and Laser Rangefinder

Flight Environment	Detection Range (m)																											
	Ultrasonic RF										Infrared RF										Laser RF									
	1	2	3	4	5	6	7	8	9	10	1	2	3	4	5	6	7	8	9	10	1	2	3	4	5	6	7	8	9	10
Sunny	√	√	√	√	√	√	√	X	X	X	√	√	√	X	X	X	X	X	X	X	√	√	√	√	√	√	X	X	X	X
Cloud	√	√	√	√	√	√	√	X	X	X	√	√	√	X	X	X	X	X	X	X	√	√	√	√	√	√	√	√	X	X
Night	√	√	√	√	√	√	√	X	X	X	√	√	√	X	X	X	X	X	X	X	√	√	√	√	√	√	√	√	√	√

4.3 Obstacle Detection Range in Different Environments Test

While an ultrasonic rangefinder is generally unaffected by its environment (such as illumination, brightness, and weather), it is tested to confirm its function in a variety of conditions. The infrared and laser rangefinders' functionality will be impacted by the illumination conditions in the environment. In bright flight situations, the average illuminance on the surface of the obstacle is between 32 Klux and 100 Klux, whereas in cloudy flight environments, the average illuminance on the surface of the obstacle is between 1 Klux and 20 Klux. Needless to add, the average value of illuminance on the surface of obstacles during night flight conditions is less than 1 lux. Table 4 summarizes the findings.

According to Table 3, the ultrasonic rangefinder can detect obstacles from 1m to 7m in various flight situations. Also, because ultrasonic rangefinders use air to measure distances between themselves and obstacles, the weather does not affect their effectiveness. The performance of the laser rangefinder varies with flight conditions since the surface of the barrier is illuminated differently in different flight situations. The laser rangefinder has a 6 m obstacle detection range in sunny conditions, 8 m in overcast conditions, and 10 m in night flight. The obstacle detection ranges of a laser rangefinder increase with decreasing surface illuminance. Nevertheless, the laser rangefinder's obstacle detection range in Table 1 matches its performance during night flight.

The infrared rangefinder's performance does not match the criteria in Table 1, which only identifies obstacles 1 to 3 meters away. Surprisingly, the degree of illuminance does not impact the infrared rangefinder's effectiveness in sunny, overcast, or night flight conditions. This is true for this particular infrared rangefinder device. The chosen ultrasonic and laser rangefinders are suited for obstacle identification in the X- and Y-axis of the multirotor aircraft frame because they can identify obstacles at a distance. The ultrasonic rangefinder also offers a larger obstacle detecting area, increasing the success rate of the collision avoidance system. Due to the design of the multirotor aircraft's frame, the infrared rangefinder can be employed for obstacle detection in the Z-axis. The Z-axis multirotor aircraft outermost components are the battery and landing gear, whereas the X- and Y-axis outermost components are the propellers.

4.4 Collision Avoidance Reaction Time Test

The reaction time of a multirotor aircraft is the time it takes to avoid an obstacle. Preventing collisions requires quick response from multirotor aircraft when obstacles are detected. This experiment is designed to estimate the reaction time of a multirotor aircraft so that it can react quickly when an obstruction is detected. Table 5 shows the results.

Table 5 shows that when travelling at 2 m/s, the multirotor aircraft reacts promptly when an obstruction is detected. However, at 4 m/s, the multirotor aircraft made evasive maneuvers 30 milliseconds after recognizing the obstruction. The multirotor aircraft also experienced a 35 milliseconds delay before performing evasive moves when going at 6 m/s.

When an obstruction is detected, the multirotor aircraft's reaction time is sufficient to avoid it. Rangefinders also read distances at 100 Hz, or 10 milliseconds each reading. As a result, the reaction time for the multirotor aircraft is 0–35 milliseconds. That's because the laser rangefinder's maximum obstacle detection range in diverse flight conditions is 6 meters, so the multirotor maximum speed is limited. It will also be unable to avoid a collision with an obstruction if it exceeds 6 m/s.

4.5 3D Collision Avoidance Test

The multirotor aircraft should be able to avoid obstacles on the X, Y, and Z axes. Figure 8 (a) shows the intended autonomous mission flight path with an impediment noted in red. The

multirotor aircraft must also avoid an impediment at waypoint 3 on the map upon landing. The mission speed for the multirotor aircraft is set to 1 m/s and the altitude to 2.5 m. Table 6 contains the results seen in Fig. 8(b)–(d).

Table 5: Collision avoidance reaction time test results

Velocity of multirotor aircraft (m/s)	Reaction time of multirotor aircraft (1 x 10^{-3} s)
2	0
4	30
6	35

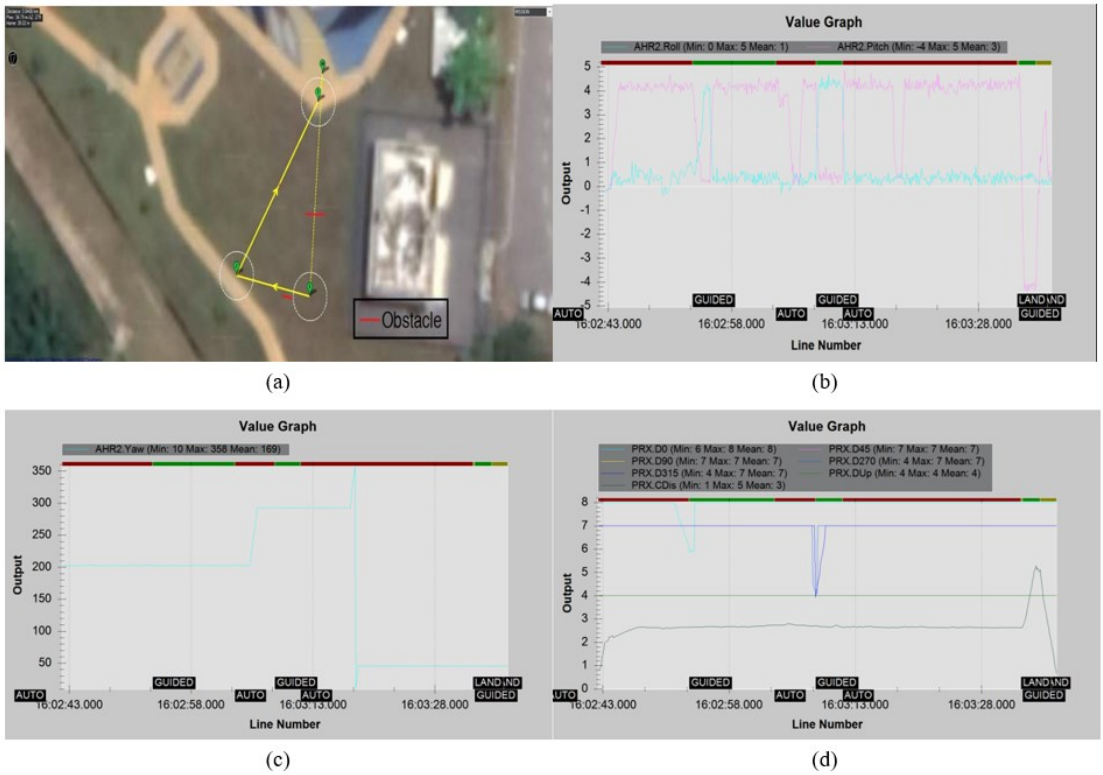

(a) (b) (c) (d)

Fig. 8: (a) Autonomous mission flight path with obstacle position marker (b) Roll and pitch angle data logged of multirotor aircraft (c) Yaw angle data logged of multirotor aircraft (d) Rangefinders data logged of multirotor aircraft

Table 6: 3D Collision Avoidance Test Results

Position of obstacle	Observation
Along X-axis	Successful avoidance
Along Y-axis	Successful avoidance
Along Z-axis	Successful avoidance

Figure 8(b) and 8(c) show the multirotor aircraft's attitude and heading reference system data logged during the autonomous mission. Moreover, positive pitch indicates forward motion, while positive roll indicates rightward motion. Also, the multirotor yaw angle shows the multirotor heading. On the other hand, Fig. 8(d) shows the rangefinder data logged during the autonomous mission, with D0 being the forward rangefinder reading, D45 the northeast

rangefinder reading, D90 the east rangefinder reading, and D315 the northwestern rangefinder reading. Also, Dup is the rangefinder reading for upwards and CDIS is the rangefinder reading for downwards. The multirotor aircraft avoided collisions along the X, Y, and Z-axis in Table 6.

To get from waypoint 0 to 1, the multirotor aircraft first pitches forward. The program for this experiment makes the multirotor aircraft conduct evasive maneuvers when it detects a forward obstruction. The forward barrier is between waypoints 0 and 1. Also, when a multirotor aircraft detects a forward obstruction, it will roll to the right until it no longer detects the barrier and then proceed forward. The multirotor aircraft then yaws 90° and pitches forward to move from waypoint 1 to 2. The back obstacle is also parallel to the path from waypoint 1 to 2. When a multirotor aircraft detects a rear obstacle, it is programmed to roll away from it and pitch ahead. To proceed from waypoint 2 to waypoint 3, the multirotor aircraft must yaw for roughly 120° and pitch forward. Also, when the multirotor aircraft reaches waypoint 3, it immediately enters LAND mode. An obstacle is positioned at waypoint 3 underneath the multirotor aircraft, which will undertake evasive maneuvers, such as pitching backward, until the object is not spotted, then land. Thus, the multirotor aircraft can avoid obstacles on the X, Y, and Z axes.

5. CONCLUSIONS

The 3D UAV collision avoidance system has been built and tested. The 3D collision avoidance system can also detect several material types and opacities in varied flight environments by combining selected rangefinders. Finally, the 3D collision avoidance algorithm can react quickly to obstructions in the X, Y, and Z axes.

In the future, the hexa-rotor design can be improved with better obstacle detection systems such as 360° LIDAR and solid-state LIDAR, or vision-based obstacle detection systems such as stereo cameras and depth sensors. As obstacle detection coverage and performance improve, better collision avoidance algorithms can be built. Suitable filters should also be attached to the obstacle detection system to eliminate inconsistent readings owing to electrical disturbances and sensor interference.

ACKNOWLEDGMENTS

The authors would like to thank Ministry of Higher Education (MOHE) for sponsoring this work under the grant no. FRGS/1/2022/TK07/UTEM/02/19. We wish to express our gratitude to honorable University, Universiti Teknikal Malaysia Melaka (UTeM) and Ministry of Higher Education (MOHE). Special appreciation and gratitude especially for Universiti Teknologi Malaysia (UTM) KL Campus, Malaysia-Japan International Institute of Technology (MJIIT), Fakulti Teknologi Kejuruteraan Elektrik dan Elektronik (FTKEE) and Underwater Technology Research Group (UTeRG), Center for Robotics and Industrial Automation (CERIA) and Ministry of Higher Education (KPT) for supporting this research.

REFERENCES

[1] Shokirov R, Abdujabarov N, Jonibek T, Saytov K, Bobomurodov S. (2020) Prospects of the development of unmanned aerial vehicles (UAVs). Tech. Sci. Innov., 2020(3): 4-8. doi: 10.51346/tstu-01.20.3-77-0069.

[2] Shakhatreh H, Sawalmeh AH, Al-Fuqaha A, Dou Z, Almaita E, Khalil I, Othman NS, Khreishah A, Guizani M. (2019) Unmanned aerial vehicles (UAVs): A survey on civil applications and key research challenges. IEEE Access, 7:48572–48634. doi: 10.1109/ACCESS.2019.2909530.

[3] Ke Y, Wang K, Chen BM. (2018) Design and implementation of a hybrid UAV with model-based flight capabilities. IEEE/ASME Trans. Mechatronics, 23(3): 1114-1125. doi: 10.1109/TMECH.2018.2820222.
[4] Magree D, Mooney JG, Johnson EN. (2014) Monocular visual mapping for obstacle avoidance on UAVs. J. Intell. Robot. Syst. Theory Appl., 74(1-2): 17-26. doi: 10.1007/s10846-013-9967-7.
[5] Ferrera E, Alcántara A, Capitán J, Castaño AR, Marrón PJ, Ollero A. (2018) Decentralized 3D collision avoidance for multiple UAVs in outdoor environments. Sensors (Basel), 18(12): 1-20. doi: 10.3390/s18124101.
[6] Eduardo Ferrera PJM, Capitan J, Castano AR. (2017) Decentralized safe conflict resolution for multiple robots in dense scenario. Rob. Auton. Syst., 91: 179-193.
[7] Harun MH, Abdullah SS, Aras MSM, Bahar MB. (2022) Sensor fusion technology for unmanned autonomous vehicles (UAV): A review of methods and applications. IEEE International Conference on Underwater System Technology: Theory and Applications (USYS), 2020:1-8.
[8] Harun MH, Abdullah SS, Aras MSM, Bahar MB. (2021) Collision avoidance control for unmanned autonomous vehicles (UAV): Recent advancements and future prospects. Indian Journal of Geo Marine Sciences, 50(12): 873-883.
[9] Sarin P. (2013) DigitalLab Course Project EP 315, 1–22.
[10] Hughes R. (2019) Amazon fires: What's the latest in Brazil?, BBC (Oct, 2019).
[11] Administration FA. (2000) Aerodynamics of flight, Pilot Handbook Aeronautic Knowledge.
[12] Hibbeler RC. (2013) Engineering Mechanics Statics, Thirteenth Edition.
[13] Hibbeler RC. (2012) Engineering Mechanics Dynamics, Thirteenth Edition.
[14] Pikalov S, Azaria E, Sonnenberg S, Ben-Moshe B, Azaria A. (2021) Vision-less sensing for autonomous micro-drones. Sensors, 21(16):5293.
[15] Hamaza S, Georgilas I, Heredia G, Ollero A, Richardson T. (2020) Design, modeling, and control of an aerial manipulator for placement and retrieval of sensors in the environment. J. F. Robot., 37(7):1224–1245.
[16] Suprapto BY, Heryanto MA, Suprijono H, Muliadi J, Kusumoputro B. (2018) Design and development of heavy-lift hexacopter for heavy payload. International Seminar on Application for Technology of Information and Communication (iSemantic), 2018-January:242–246. doi: 10.1109/ISEMANTIC.2017.8251877.
[17] Ahmed MDF, Mohanta JC, Zafar MN. (2018) Development of smart quadcopter for autonomous overhead power transmission line inspections. Materials Today: Proceedings, 51:261-268.
[18] Zhao T. (2018) Propulsive battery packs sizing for aviation applications. Master Theses.